LOS ALAMOS SCIENTIFIC LABORATORY
of the
UNIVERSITY OF CALIFORNIA

Report written:
May 7, 1953

LA-1552

This document consists of 22 pages
No. ____ of 147 copies, Series A

ANGULAR DISTRIBUTION OF FRAGMENTS FROM NEUTRON-INDUCED FISSION

by

J. E. Brolley, Jr.
W. C. Dickinson

PHYSICS AND MATHEMATICS

4/8/57

RESTRICTED DATA

This document contains restricted data as defined in the Atomic Energy Act of 1946. Its transmittal or the disclosure of its contents in any manner to an unauthorized person is prohibited.

PHYSICS AND MATHEMATICS

Distributed: AUG 10 1956

LA-1552

Los Alamos Report Library	1-20
AF Plant Representative, Burbank	21
AF Plant Representative, Seattle	22
ANP Project Office, Fort Worth	23
Argonne National Laboratory	24-31
Armed Forces Special Weapons Project (Sandia)	32
Armed Forces Special Weapons Project, Washington	33
Army Chemical Center	34
Atomic Energy Commission, Washington	35-37
Battelle Memorial Institute	38
Bechtel Company	39
Brookhaven National Laboratory	40-42
Bureau of Ships	43
California Research and Development Company	44-45
Carbide and Carbon Chemicals Company (C-31 Plant)	46-47
Carbide and Carbon Chemicals Company (K-25 Plant)	48-49
Carbide and Carbon Chemicals Company (ORNL)	50-55
Carbide and Carbon Chemicals Company (Y-12 Plant)	56-59
Chicago Patent Group	60
Chief of Naval Research	61
Columbia University (Havens)	62
Commonwealth Edison Company	63
Department of the Navy - Op-362	64
Detroit Edison Company	65
Directorate of Research (WADC)	66
duPont Company, Augusta	67-69
Foster Wheeler Company	70
General Electric Company (ANPP)	71-73
General Electric Company, Richland	74-77
Hanford Operations Office	78
Idaho Operations Office	79-82
Iowa State College	83
Knolls Atomic Power Laboratory	84-87
Mallinckrodt Chemical Works	88
Massachusetts Institute of Technology (Kaufmann)	89
Monsanto Chemical Company	90
Mound Laboratory	91-93
National Advisory Committee for Aeronautics, Cleveland	94
National Bureau of Standards	95
Naval Medical Research Institute	96
Naval Research Laboratory	97-98
New Brunswick Laboratory	99
New York Operations Office	100-101
North American Aviation, Inc.	102-104
Nuclear Development Associates, Inc.	105
Patent Branch, Washington	106
Pioneer Services Engineering Company	107
RAND Corporation	108
Sandia Corporation	109
Savannah River Operations Office, Augusta	110
USAF-Headquarters	111
USAF Resident, East Hartford	112
U.S. Naval Radiological Defense Laboratory	113
UCLA Medical Research Laboratory (Warren)	114
University of California Radiation Laboratory, Berkeley	115-119
University of California Radiation Laboratory, Livermore	120-122
University of Rochester	123-124
Vitro Corporation of America	125-126
Walter Kidde Nuclear Laboratories, Inc.	127
Westinghouse Electric Corporation	128-131
Yale University	132
Technical Information Service, Oak Ridge	133-147

ABSTRACT

The angular distribution of fission fragments from the neutron-induced fission of several isotopes has been studied. Distributions were observed for thermal neutrons on U^{233} and U^{235}, Lady Godiva leakage neutrons on U^{235} and U^{238}, and 14 Mev neutrons on U^{233}, U^{235}, U^{238}, Th^{232}, and Np^{237}. No anisotropy was observed for thermal neutron fission, whereas for Lady Godiva neutrons and 14 Mev neutrons the probability of fission along the axis of the neutron beam was determined to be higher than for fission in the orthogonal direction. Experimental results are given on pages 10 and 11.

ACKNOWLEDGMENT

The authors wish to thank the personnel of Groups P-2, W-2, and P-4 for the use of their equipment. In particular, we thank R. E. Peterson of W-2 and R. W. Davis and A. H. Frentrop of P-4 for considerable aid in the installation of our apparatus and the taking of data. Thanks are due to J. Povelites for the preparation of the fission foils. We are indebted to K. Boyer for suggesting the type of collimator used in these experiments and to D. L. Hill for several interesting interpretative discussions.

CONTENTS

1. Introduction

The Bohr-Wheeler liquid drop model for the fission process[1] would predict essentially no correlation between the direction of the incoming fast neutron and the direction of the fission fragments, apart from center-of-mass effects. According to this model, the energy of the neutron is quickly assimilated among the individual nucleons of the fissionable nucleus and only later is this energy concentrated on a mode of deformation leading to fission. However, according to the new collective model for the fission process formulated by Hill and Wheeler,[2] part of the energy of the incoming fast neutron goes to nucleonic excitation and part to vibrational excitation of the nuclear surface. The vibrational excitation will be predominantly such as to distort the nucleus along the direction of the neutron beam, leading preferentially to fission in this direction. It is also possible that the presence of a nuclear quadrupole moment would influence the angular distribution, since a nucleus that is elongated in prolate form might be expected to fission more readily in the direction of the long axis.

We have measured the angular distribution of the fragments from the 14 Mev neutron-induced fission of several isotopes to provide a test between these two pictures of the fission process. We have observed also the angular distribution of fragments from thermal neutron-induced fission. This was done principally to provide a check of our experimental apparatus since no anisotropy would be expected from any reasonable picture of the fission process.

In addition, we have observed the angular distribution of fission fragments using neutrons closely approximating those from a fission spectrum. This information might be of interest in bomb physics. It is known that prompt fission neutrons are more intense along the axis of fission fragment motion than in the orthogonal direction.[3] Hence, an anisotropic distribution of the fission fragments would indicate that there is a correlation function between the neutron which induces fission and the resulting fission neutrons.

2. Apparatus

2.1 Fission Chamber

Figure 1 is a photograph of the fission chamber with the cover removed. Figure 2 is a schematic representation of the chamber illustrating the type of collimation which was employed. The negative high-voltage electrode was honeycombed with 0.040 inch holes drilled on a hexagonal matrix to fill a circle 1 inch in diameter. These passages were inclined 45°

1. N. Bohr and J. A. Wheeler, Phys. Rev. 56, 426 (1939).
2. D. L. Hill and J. A. Wheeler, Phys. Rev. 89, 1102 (1953).
3. J. S. Fraser, Phys. Rev. 88, 536 (1952).

with respect to the normal in order that the geometry would be in all essentials identical for the 0^{o} and 90^{o} angular settings. No geometrical or shadowing corrections are necessary when this scheme is used. The length of the collimator holes was 0.382 inch, resulting in an extreme angular resolution of $\pm 6^{o}$ and an average angle of emission of the fragments of approximately $2\text{-}1/2^{o}$ from the axis of collimation. Thickness of the walls separating the collimator holes was 0.006 inch; geometrical transmission of the collimator was 68 percent. The collector electrode was mounted on three 1 inch long steatite insulators and the negative high-voltage electrode was separated from the collector electrode also by three 1 inch long steatite insulators. The high voltage lead was insulated with a teflon tube. A gas filling of 95 percent argon and 5 percent CO_2 was used at a pressure of 45 cm Hg so that the fastest fission fragments would be stopped shortly before reaching the collector. A negative voltage of 300 volts obtained from a dry battery was applied to the collimator electrode and the collector electrode was connected directly to the grid (1 megohm grid leak) of the first tube of a preamplifier held on the back of the fission chamber so as to make a shielded unit. No attempt was made to attain saturation. The rise time of the electron collection pulses was about 0.5 μsec. The chamber was mounted so that it could be rotated by means of an indexed rotary table about an axis containing a diameter of the fissionable layer. Angular error of position probably did not exceed 0.5^{o}. A cadmium jacket surrounded the chamber when thermally fissionable materials were being studied with fission-spectrum or 14 Mev neutrons.

2.2 Electronic Equipment

A Los Alamos Model 130 preamplifier was attached to the back of the fission chamber. This preamplifier has a gain of approximately 50 and a cathode follower output which transmits signals via a long 93 ohm cable to a Los Alamos 101A amplifier with a rise time of 0.5 μsec and an RC clipping time of 2 μsec. With this clipping time no large pulses caused by alpha-particle pile-up were ever observed. In most of the experiments two Los Alamos Model 700 scalers were driven in parallel by the amplifier. The discriminator setting of one scaler was such as to accept all fission pulses while the discriminator setting of the second scaler was such as to accept principally only pulses from the higher energy (light) fragments. (See Sections 3.1 and 3.3). Data in some of the later experiments at the Cockcroft Walton were taken with the Cockcroft-Walton 18 channel pulse-height analyzer attached to the output of the amplifier.

The linearity and amplification of the equipment were checked periodically during the experiments with a Los Alamos Model 500 precision pulse generator.

2.3 Fission Foils

Thin layers of U_3O_8, NpO_2, and ThO_2 were prepared by J. Povelites by painting solutions of the nitrates on 10 mil platinum discs and baking at 800°C until the oxides were formed. Deposits ranging from 100 $\mu g/cm^2$ to 5 mg/cm^2 were used. Table 1 gives approximate analyses of the foils.

TABLE 1

Principal Element	% Principal Element
Th^{232}	100
U^{233}	96 (balance normal U)
U^{235}	95.7 (1/2% U^{234}, balance U^{238})
U^{238}	(16 parts per million of U^{235})
Np^{237}	100

2.4 Neutron Sources

2.4.1 Water Boiler. The south thermal column of the Water Boiler furnished a steady, well collimated beam of thermal neutrons. A bismuth filter between the reactor and the graphite column attenuated the gamma rays. Resulting gamma ray intensity was quite low and the amount of photofission would be insignificant. A steel collimator with a 2.37 inch diameter circular aperture was used. The wall of the reactor was covered with cadmium sheet to exclude extraneous thermal neutrons. By means of a small U^{235} spiral fission counter, the neutron intensity across the beam was found to be flat to better than 1 percent. For these studies the Water Boiler ran at a 30 kw power level. Figure 3 is a photograph of the south face of the Water Boiler with the fission chamber in place.

2.4.2 Lady Godiva. The leakage neutron spectrum from Lady Godiva is closely similar to a pure fission spectrum from slightly less than 1 Mev up to the maximum, according to preliminary studies of L. Rosen. Production of gamma rays was copious but photofission was again probably not significant. The center of the U^{235} sphere was 75 inches from the concrete floor. The fission chamber was aligned so that the perpendicular line passing through the center of a fission foil went through the center of the glory hole of Lady Godiva. The plane of the fission foils was 26-1/2 inches from the center of the sphere. A power level of about 100 watts was maintained during the measurements.

Degradation of the leakage spectrum at the position of our chamber caused by scattering from surrounding material has been determined by R. E. Peterson and G. A. Linenberger

of Group W-2 and found to be small. Using a spiral fission chamber, they found that the relative counting rate for U^{238} followed closely an r^{-2} dependence out to 29 inches from the center of Lady Godiva. For U^{235} the (no cd)/(cd) counting rate ratio at 6 inches from the center was 1.12, whereas at 29 inches from the center it was 3.9. This corresponds to only a fraction of 1 percent of thermal neutrons at the 29 inch position.

Because of the great distance of Lady Godiva from the control room, the instrumentation differed slightly from other installations. The 101A amplifier was located in the Kiva which housed Lady Godiva, along with two discriminators whose settings could be adjusted remotely in the control room. The outputs of the discriminators were piped from the Kiva to scalers in the control room. Figure 4 is a photograph of Lady Godiva with the fission chamber in place.

2.4.3 Cockcroft-Walton. Fourteen-Mev neutrons were produced in the Cockcroft-Walton machine by the $T(d,n)\alpha$ reaction (Q = 17.6 Mev). Deuterons, accelerated to 240 Kev and magnetically analyzed, struck an air-cooled thick zirconium foil in which tritium had been absorbed. The fission chamber intercepted neutrons emitted at 74^{o} with respect to the incident deuteron beam. These neutrons had an energy of 14.3 ± 0.1 Mev. L. Rosen has found, by use of nuclear emulsions, that about 3 percent of the emitted neutrons are of degraded energy. The plane of the fission foils was 6.25 inches from the center of the Zr-T target. The machine operated with deuteron currents of 100-150 μamp and with neutron yields up to 2×10^{10} neutrons/sec, depending on the condition of the targets which are slowly poisoned. Figure 5 is a photograph of the reaction area of the Cockcroft-Walton with the fission chamber in place.

3. Procedure for Accumulation of Data

3.1 Water Boiler

For each fission foil, it is necessary first to run an integral bias curve to ascertain proper bias settings for the two discriminators. The totality of fission fragments produces a double peaked ionization spectrum. This is illustrated in Figure 6 from the work of J. Wahl for thermal and 14 Mev neutrons (AECD-3379).

Although the valley between the two energy peaks does not go to zero, indicating an overlapping of the light and heavy particle distributions, it can be shown that the relative separation of the peaks increases from about 1.5 to about 2 because of the considerable energy loss of the fragments in the collimator before entering the sensitive volume of the chamber. Hence it would appear plausible that there is a nearly complete separation of the two ionization peaks as observed in the chamber and this seems to be confirmed by the two

flat shelves observed for the integral bias curves taken at the various installations. Figure 7 is an example of such an integral bias curve taken at the Water Boiler. The arrows indicate the bias settings of the two discriminators. It would appear that the scaler whose discriminator was set on the upper plateau would count all fragments and the scaler whose discriminator was set on the lower plateau only the light fragments. It has been found, however, from later observation of the differential pulse height spectrum and also from calculated pulse height spectra, that the two fission peaks are not completely separated and hence that the lower plateau cannot be truly horizontal. Therefore, no data are given in this report for the angular distribution of the light fragments only. More will be said about the shape of the pulse height spectra in Section 3.3.

Because the thermal neutron flux from the Water Boiler varied less than 0.5 percent over a considerable time interval, no neutron monitor was necessary. Fission counting was performed at 0°, 45°, and 90°. Approximately 2000 counts were taken at each angular setting, and 0.1 mg/cm^2 foils of $U_3^{233}O_8$ and $U_3^{235}O_8$ were used.

3.2 Lady Godiva

The integrated neutron flux was monitored by a flat U^{235} fission chamber and also by a BF_3 proportional counter surrounded by paraffin. The integrated neutron intensity as given by these two monitors always agreed within 0.5 percent. A 0.6 mg/cm^2 $U_3^{235}O_8$ foil and a 0.5 mg/cm^2 $U_3^{238}O_8$ foil were used. For U^{235} about 2000 fission counts were obtained at 0°, then 2000 counts at 90°. This procedure was repeated four times. For U^{238} about 500 counts were taken at each position. Again the procedure was repeated four times.

3.3 Cockcroft-Walton

The integrated neutron flux was monitored by counting the alpha particles generated in the $T(d,n)\alpha$ reaction by means of a proportional counter attached to the target apparatus. Also a long counter directly monitored the neutron flux. In some cases, these two monitors disagreed by as much as 2 percent. The alpha counter was always used as the standard monitor.

The two discriminator setup was used for the following foils: 1 mg/cm^2 $U_3^{233}O_8$; 1 and 5 mg/cm^2 $U_3^{235}O_8$; 0.6, 1, and 6 mg/cm^2 $U_3^{238}O_8$; and 5 mg/cm^2 $Th^{232}O_2$. A typical integral bias curve as obtained for the 1 mg/cm^2 $U_3^{233}O_8$ foil is shown in Figure 8. The 18 channel (5 volt widths) pulse height analyzer was used for the following foils: 0.7 mg/cm^2 $Np^{237}O_2$; 0.6 and 1 mg/cm^2 $U_3^{238}O_8$. A typical pulse height spectrum as obtained for the 0.6 mg/cm^2 $U_3^{238}O_8$ foil is shown in Figure 9. It is clear from this figure that the two peaks are not sufficiently separated to allow counting of only the light fragments.

Because of the center-of-mass effect for 14 Mev neutrons, a fission fragment emitted at 90^{o} will have about 3-1/2 percent less energy than if it were emitted at 0^{o}. The rather large energy loss of the fragments in the collimator of the fission chamber results in a magnification of this effect. Thus, for a 1 mg/cm^2 foil thickness, the ionization peaks were observed to shift downward about 10 percent going from the 0^{o} to the 90^{o} angular setting. This is in close agreement with the calculated value of the shift. The discriminator was always set far enough back on the upper plateau so as to count essentially all the fragments at both angular settings. Any error in the $0^{o}/90^{o}$ ratios resulting from this factor is estimated not to be greater than 1 or 2 percent.

4. Experimental Results

4.1 Thermal Neutrons

The $0^{o}/90^{o}$ fission intensity ratios for U^{233} and U^{235} were found to be 1.00 ± 0.08 and 0.99 ± 0.09, respectively.[4] The fission intensity at 45^{o} was no different within statistical error from the intensity at 0^{o} and 90^{o}.

4.2 Fission Spectrum Neutrons

The $0^{o}/90^{o}$ fission intensity ratios for U^{235} and U^{238} in the center-of-mass system were determined to be 1.06 ± 0.07 and 1.27 ± 0.11, respectively. Although the measured anisotropy for the U^{235} isotope is quite small, we feel that the effect is most probably real.

4.3 14 Mev Neutrons

Table 2 summarizes the experimental results for $0^{o}/90^{o}$ fission intensity ratios.[5, 6]

---

4. Uncertainty limits used in this report are the 95 percent confidence intervals. These are approximately three times the probable error limits or twice the standard deviation limits. The errors quoted are due to counting statistics only. We feel that systematic error is sufficiently small compared to statistical error to warrant the neglect of the former.

5. The $0^{o}/90^{o}$ ratio for neptunium was also measured at the cyclotron, using 12.8 Mev neutrons from the $D(d,n)He^3$ reaction, and gave 1.20 ± 0.13.

6. According to unpublished work of H. C. Martin of this laboratory, the fission cross-section at 14 Mev for Np^{237} is 2.3 barns. From our geometry, total neutron flux, foil weight, etc., we calculated the cross-section to be 2.8 barns. The error in our calculated value is no doubt large enough so as not to indicate any disagreement in these two values.

TABLE 2

Isotope	Type	Foil	$0^{o}/90^{o}$ Ratio (center-of-mass)	
U^{233}	Even-odd	1 mg/cm^2 U_3O_8	1.32 ± 0.11	←
U^{235}	" "	1 " "	1.27 ± 0.17	←
		5 " "	1.31 ± 0.09	
U^{238}	Even-even	0.6 " "	1.31 ± 0.12	←
		1 " "	1.24 ± 0.10	
		6 " "	1.53 ± 0.17	
Th^{232}	" "	5 " ThO_2	1.53 ± 0.21	
Np^{237}	Odd-even	0.7 " NpO_2	1.15 ± 0.09	←

We consider those ratios marked by an arrow to be terminal values for this experiment. Because of the rather large difference between the U^{238} ratios found using the 0.6 or 1 mg/cm^2 foil and the ratio resulting from use of the 6 mg/cm^2 foil, we hesitate to quote the Th^{232} ratio as terminal. Low counting rates and lack of time prevented a measurement with a thinner foil.

Angular distributions, with points at 0^{o}, 30^{o}, 60^{o}, and 90^{o}, were taken for U^{235}, U^{238}, and Th^{232} using 5 mg/cm^2, 6 mg/cm^2, and 5 mg/cm^2 foils, respectively. Since only the shape of the curves was wanted, the thicker foils were used to boost the counting rates. Figure 10 is the curve obtained for U^{235}. The experimental points in all cases could be satisfactorily fitted to a curve of the form $1 + A \cos^2\theta$, where θ is the angle between the fragment direction and the neutron beam.

5. Conclusions

These experiments clearly show that the angular distribution of fragments from fission induced by 14 Mev neutrons is anisotropic; fission parallel to the axis of the neutron beam is more probable than is fission in the orthogonal direction. In fact, the four final ratios tabulated in Table 2 indicate that the magnitude of the anisotropy at this neutron energy may well be essentially independent of the isotope. An average anisotropy of about 25 percent is obtained from these ratios. For the isotopes U^{233} and U^{235} it is evident from the Lady Godiva experiments that the effect persists to much lower neutron energies, although perhaps diminishing in magnitude. As would be expected, there is no anisotropy in the case of thermal neutrons.

Winhold, Demos, and Halpern[7] have measured the angular distribution of fission fragments in the 16 Mev photofission of Th^{232} and found a $1 + A \sin^2\theta$ dependence corresponding to a higher intensity of fission fragments at 90^o to the incident beam of photons. We observe a $1 + A \cos^2\theta$ dependence for 14 Mev neutrons. Both our results for fast neutron fission and their results for photofission are compatible with the collective model picture of the fission process. However, it is of interest to note that, whereas we find that the anisotropy probably becomes smaller (or at least no larger) with decreasing neutron energy, they find that the anisotropy increases with decreasing photon energy. The inverse dependence on energy may result, in part, from the nature of the absorptive process by which the proton in the nucleus gains energy and angular momentum from the incident photon.

7. E. J. Winhold, P. T. Demos, and I. Halpern, Phys. Rev. 87, 1139 (1952).

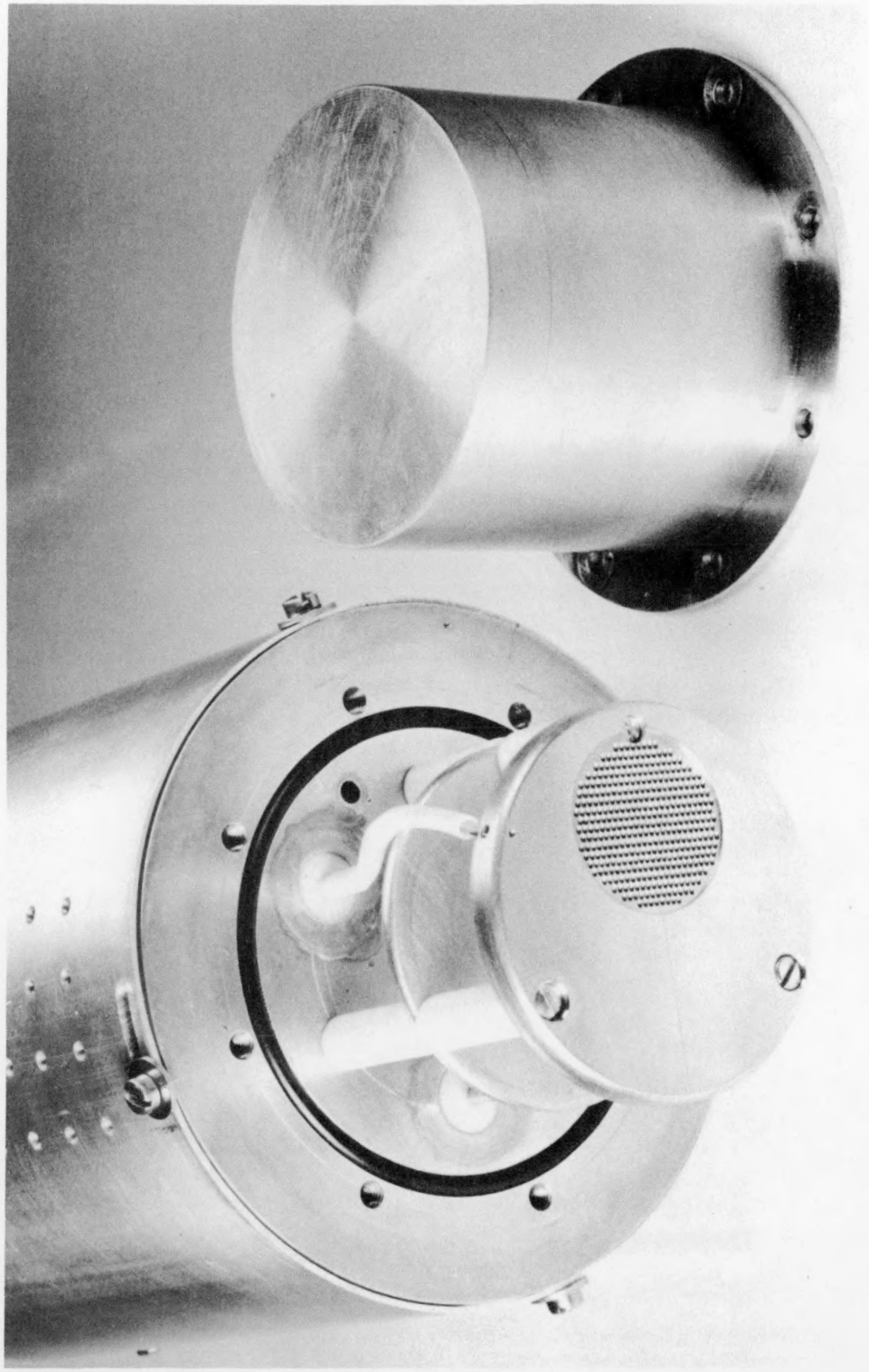

Fig. 1. The fission ionization chamber with cover removed.

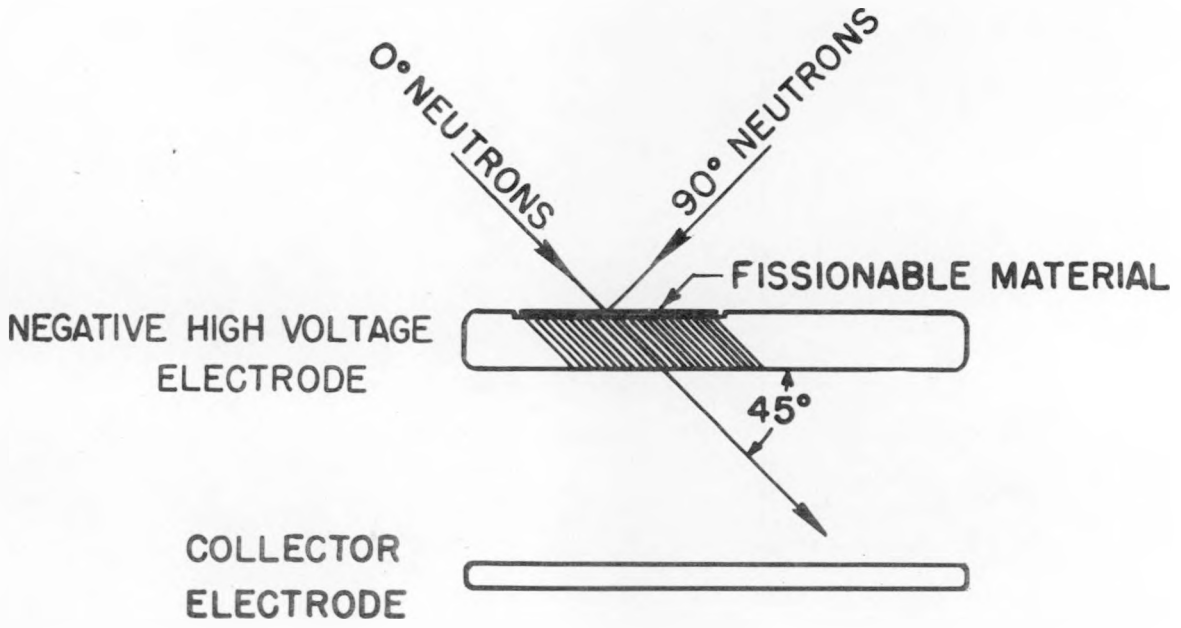

Fig. 2. Schematic representation of the fission chamber.

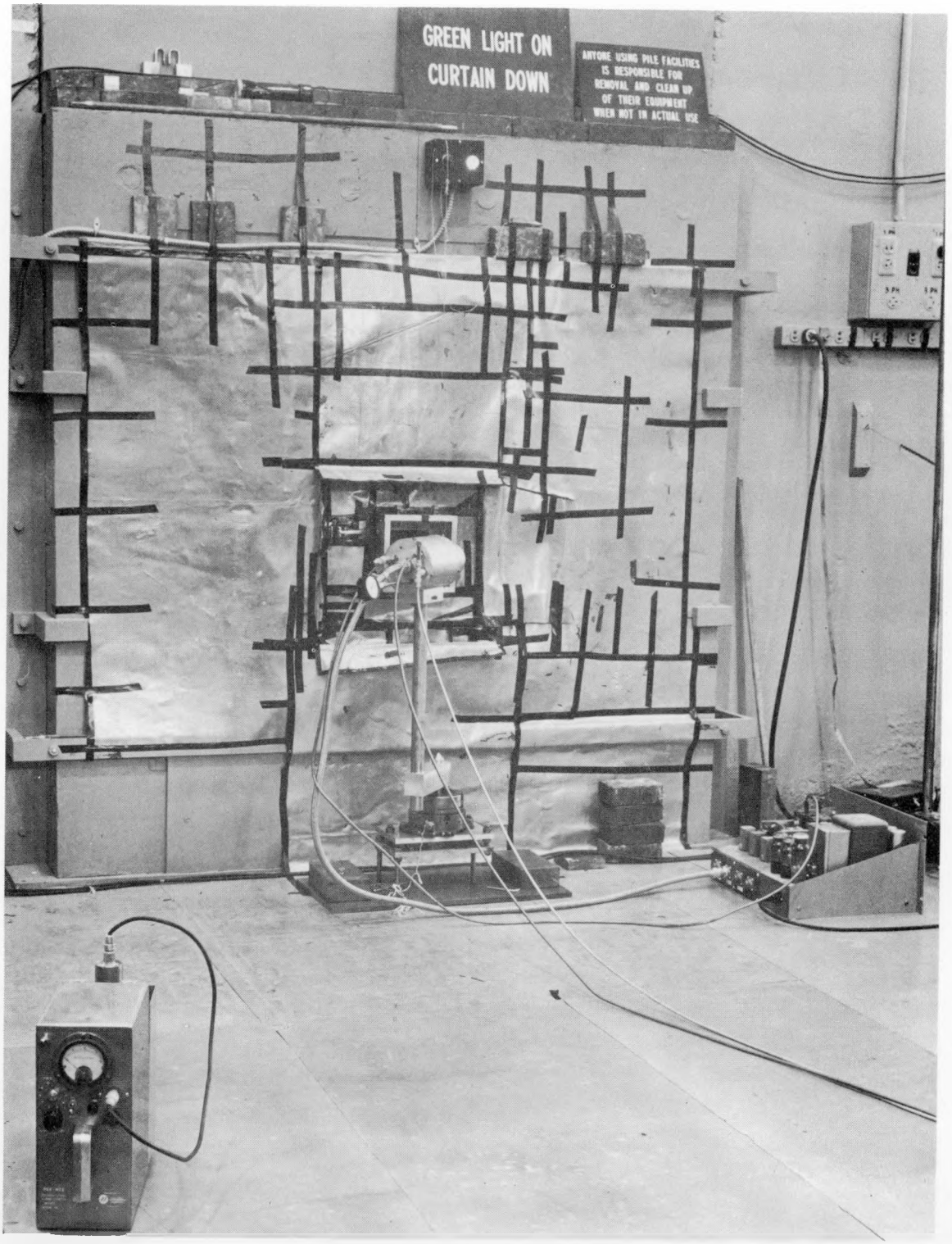

Fig. 3. The south face of the Water Boiler with fission chamber in place.

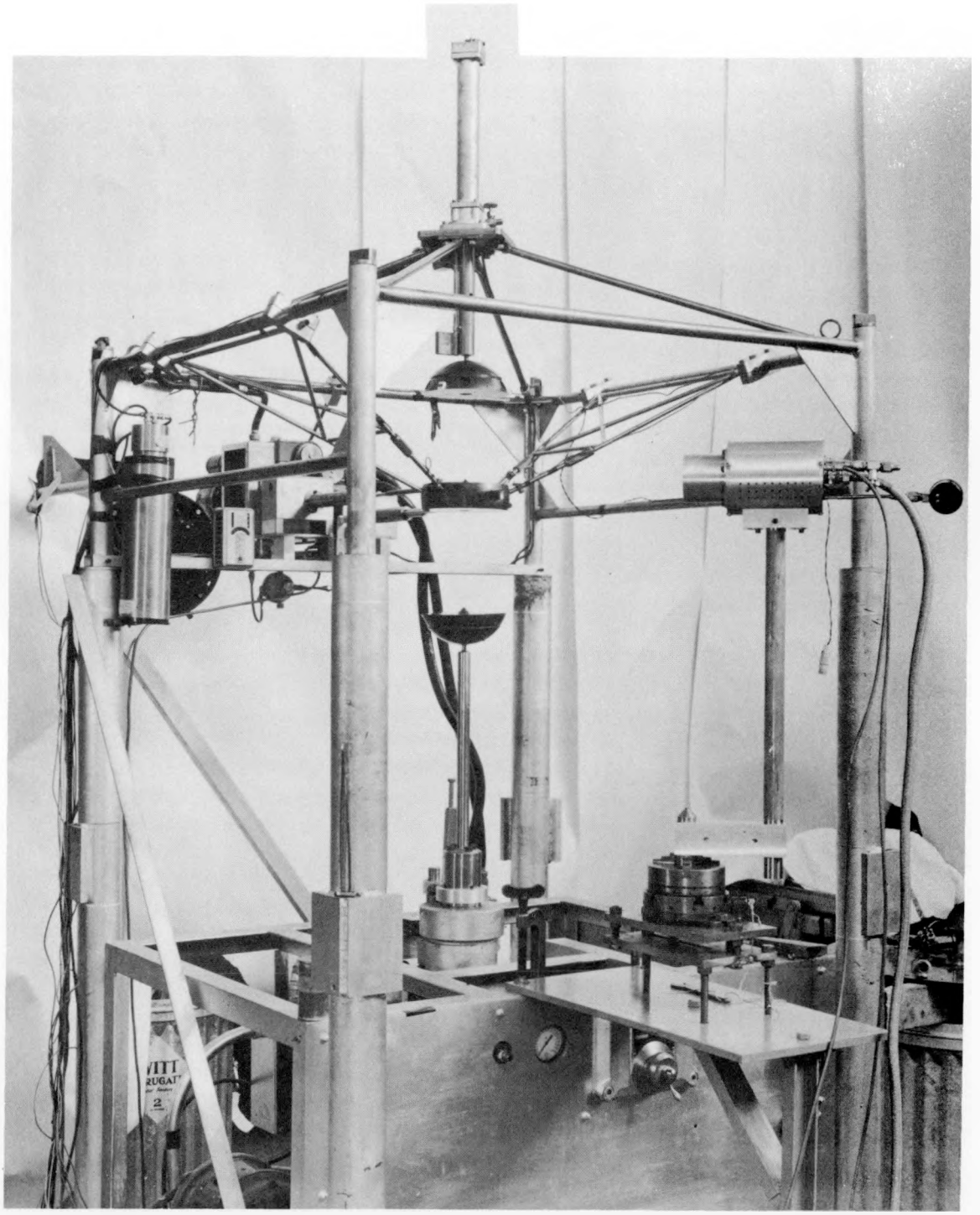

Fig. 4. Lady Godiva with fission chamber in place.

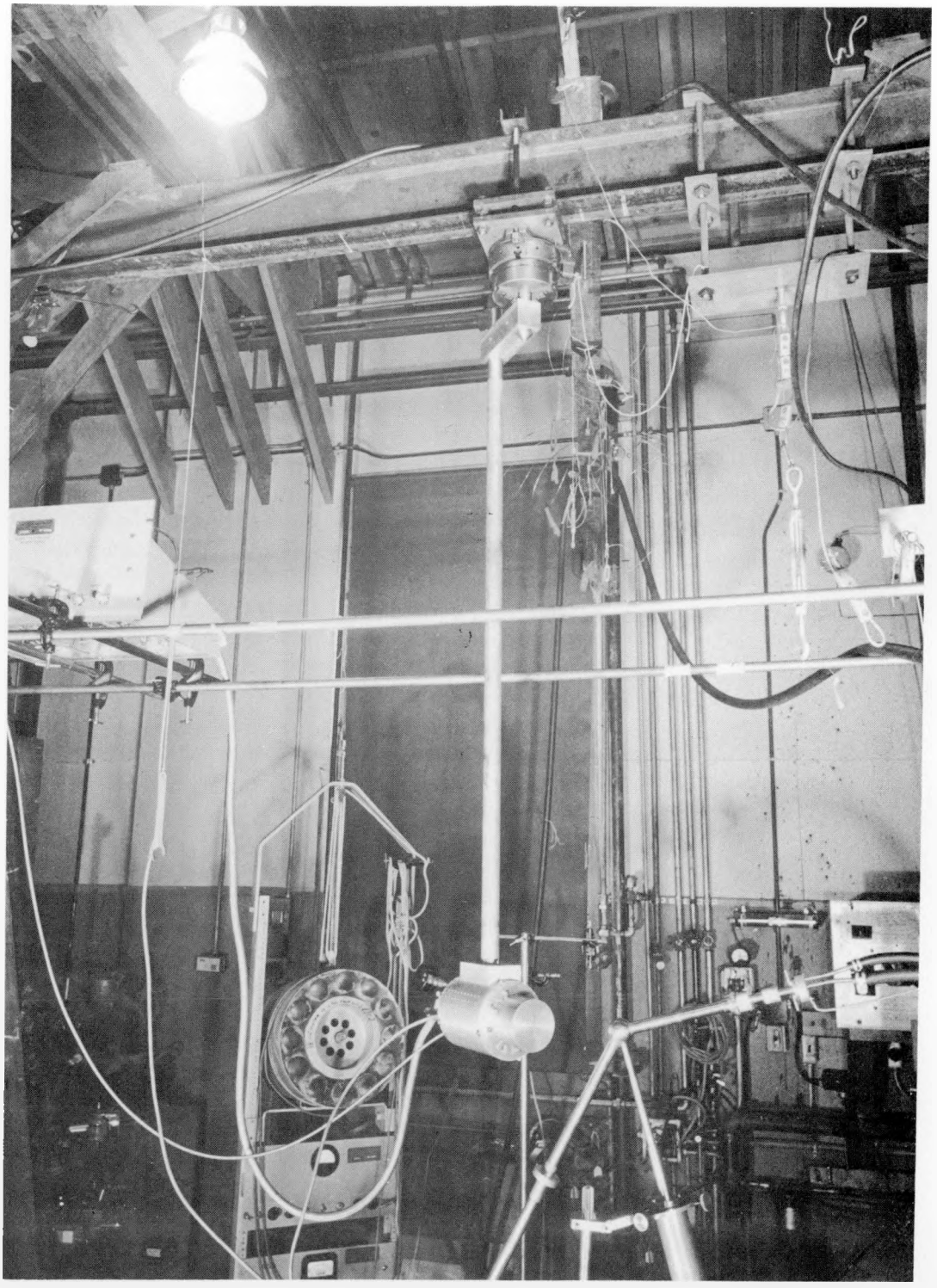

Fig. 5. Reaction area of Cockcroft Walton with fission chamber in place.

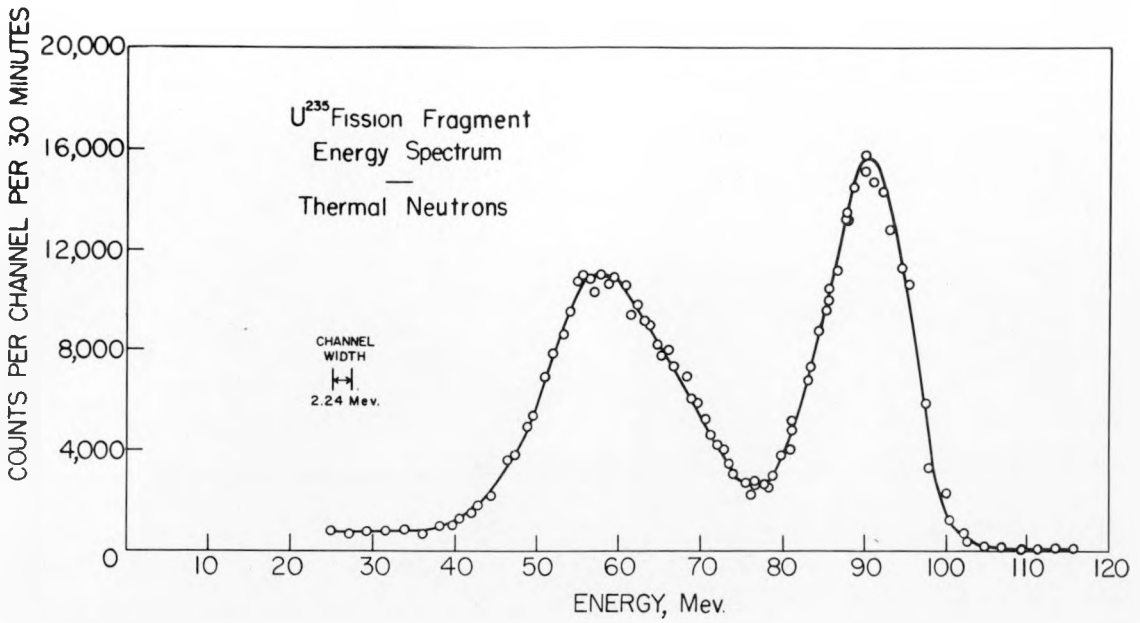

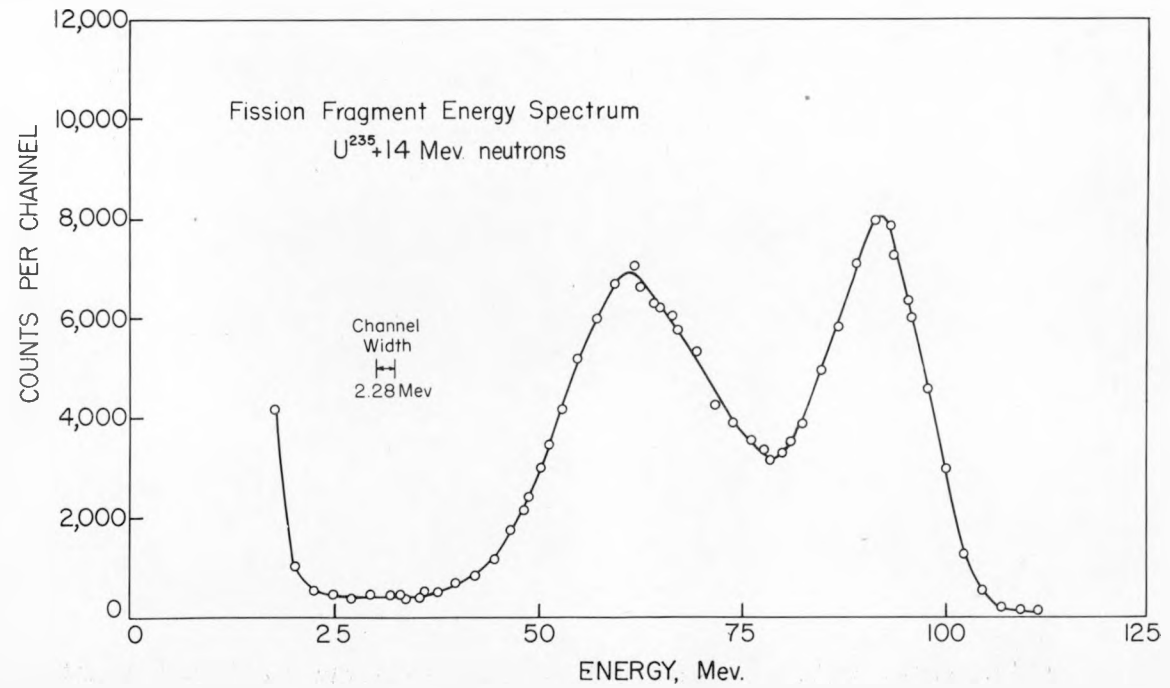

Fig. 6. Fission fragment energy spectra for thermal and 14-Mev neutrons.

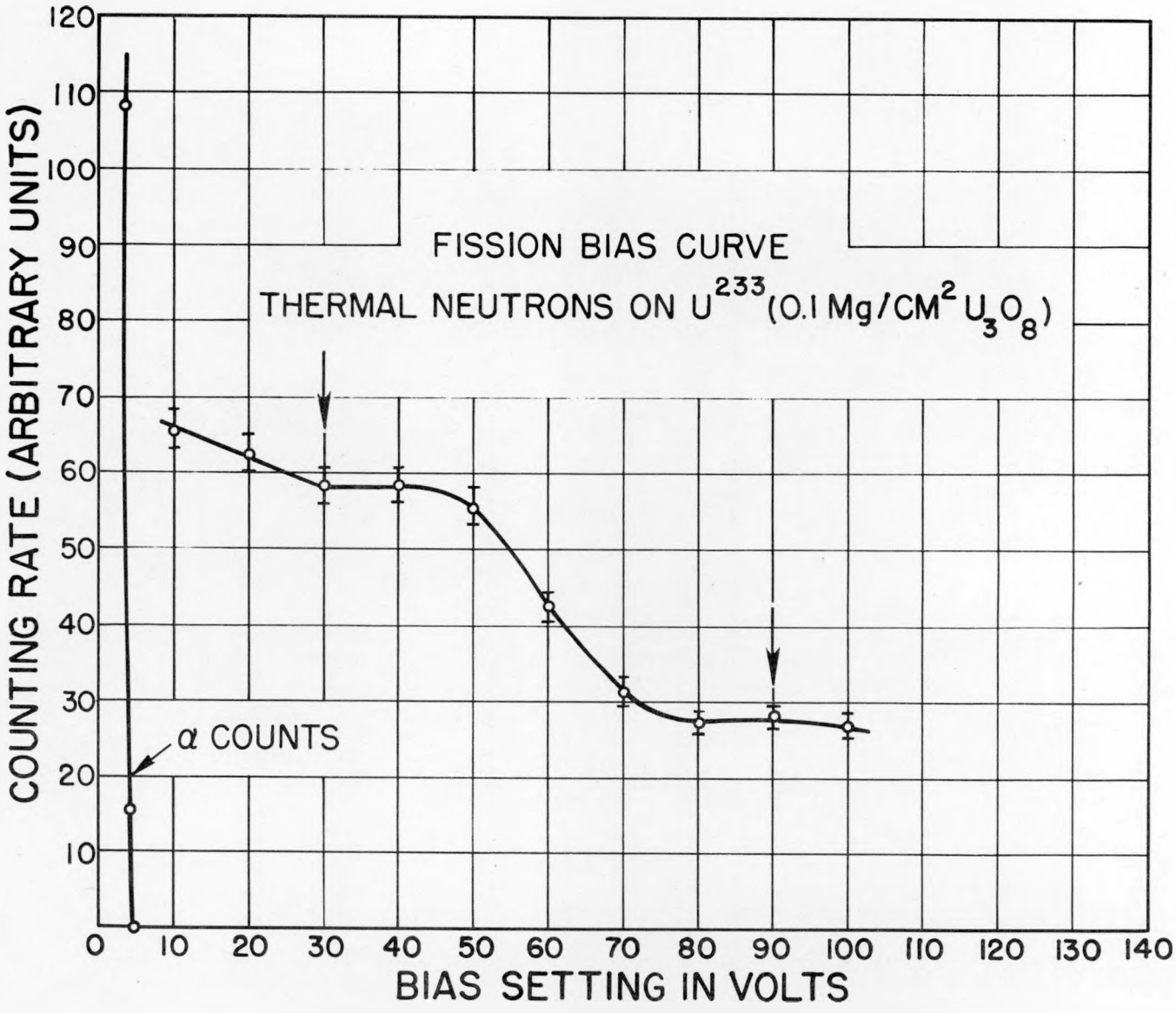

Fig. 7. An integral bias curve taken with thermal neutrons.

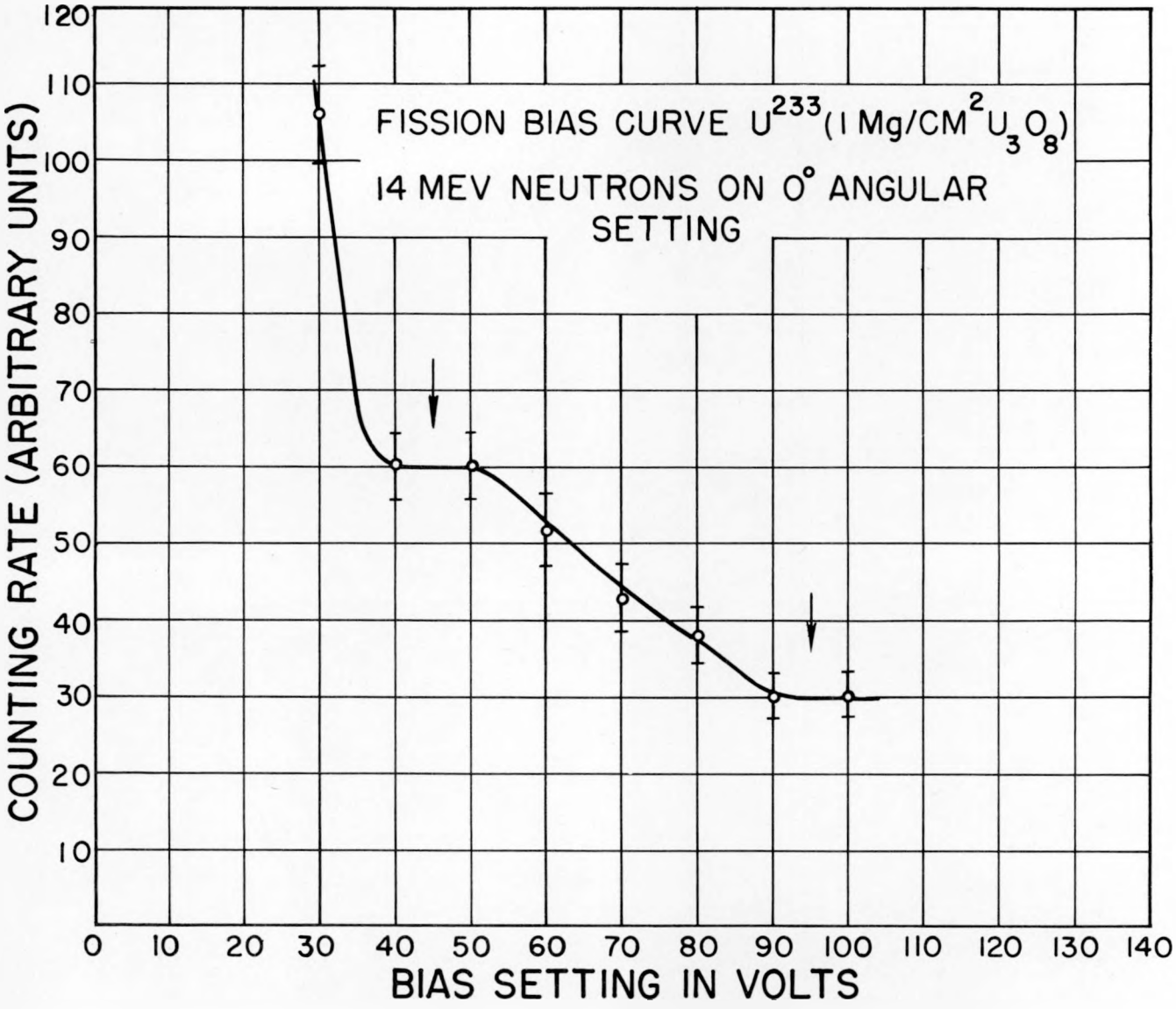

Fig. 8. An integral bias curve taken with 14-Mev neutrons.

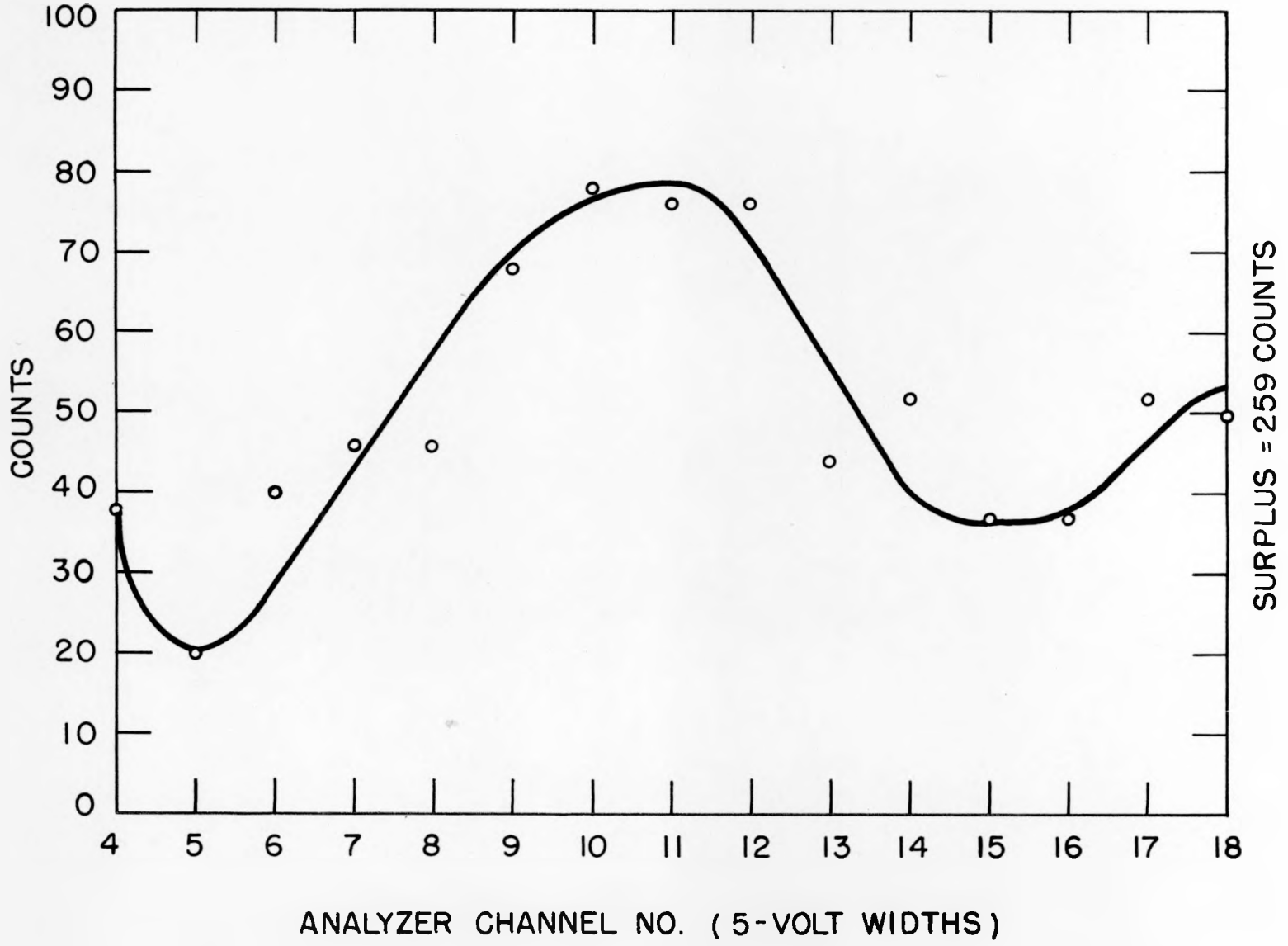

Fig. 9. A pulse height spectrum taken with 14-Mev neutrons.

CONFIDENTIAL SECURITY INFORMATION

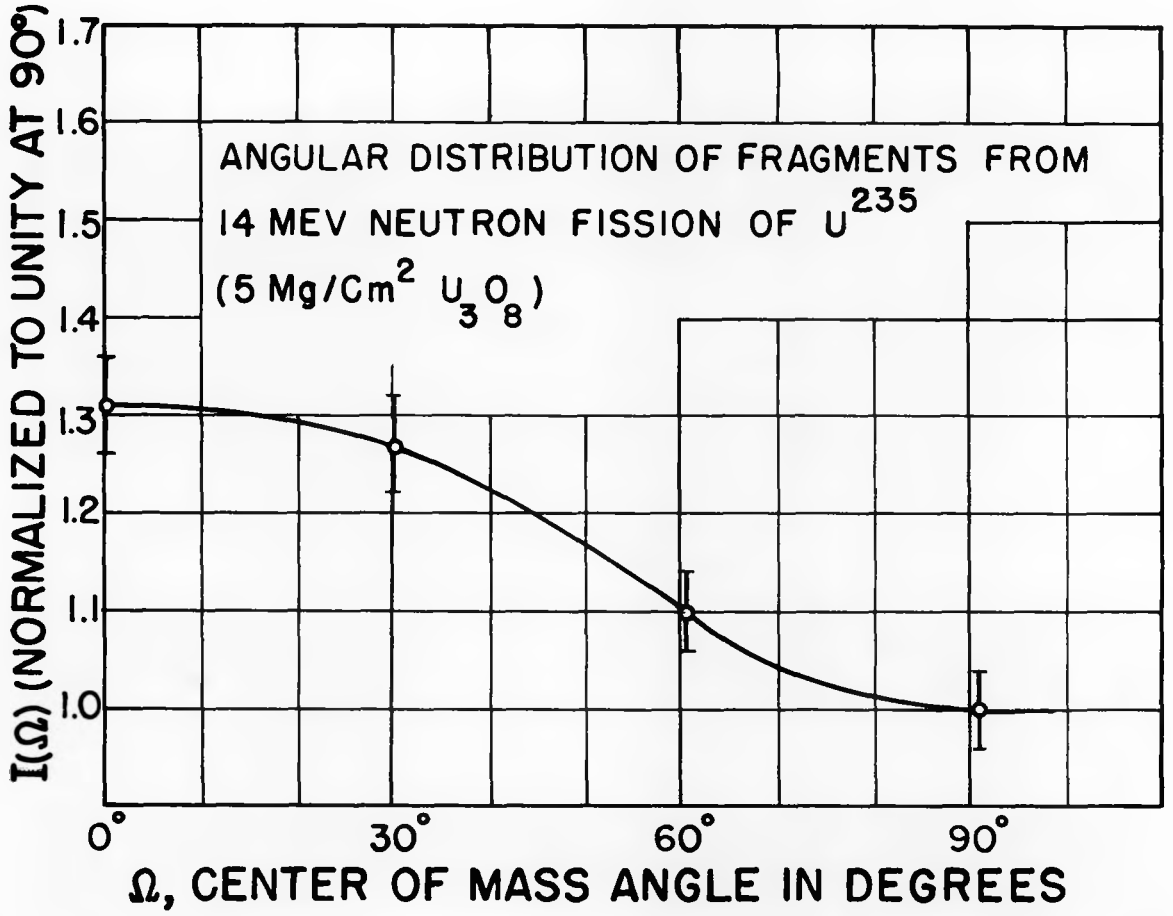

Fig. 10. Angular distribution of fragments from the 14-Mev fission of U^{235}.

CONFIDENTIAL SECURITY INFORMATION